

Seafloor sediment characterization improves estimates of organic carbon standing stocks: an example from the Eastern Shore Islands, Nova Scotia, Canada

Catherine Brenan¹, Markus Kienast¹, Vittorio Maselli², Christopher K. Algar¹, Benjamin Misiuk^{3,4}, Craig J. Brown¹

5 ¹Department of Oceanography, Dalhousie University, Halifax, B3H 4R2, Canada

²Department of Chemical and Geological Sciences, University of Modena and Reggio Emilia, Modena, Italy

³Department of Geography, Memorial University of Newfoundland, St. John's, A1B 3X9, Canada

⁴Department of Earth Sciences, Memorial University of Newfoundland, St. John's, A1B 3X9, Canada

10

Corresponding Author: Craig J. Brown (craig.brown@dal.ca)

Abstract. Continental shelf sediments contain some of the largest stocks of organic carbon (OC) on Earth and play a vital role in influencing the global carbon cycle. Quantifying how much OC is stored in shelf sediments and determining its residence time is key to assessing how the ocean carbon cycle will be altered by climate change and possibly human activities. Spatial variations in terrestrial carbon stocks are well studied and mapped at high resolutions, but our knowledge of the distribution of marine OC in different seafloor settings is still very limited, particularly in dynamic and spatially variable shelf environments. This lack of knowledge reduces our ability to understand and predict how much and for how long oceans sequester CO₂. In this study, we use high-resolution multibeam echosounder (MBES) data from the Eastern Shore Islands offshore Nova Scotia (Canada), combined with OC measurements from discrete samples, to assess the distribution of OC content in seafloor sediments. We derive four different spatial estimates of organic carbon stock: i) OC density estimates scaled to the entire study region assuming a homogenous seafloor; ii) interpolation of OC density estimates using Empirical Bayesian Kriging; iii) OC density estimates scaled to areas of soft substrate estimated using a high-resolution classified substrate map; and finally, iv) Empirical Bayesian Regression Kriging of OC density within areas of estimated soft sediment only. These four distinct spatial models yielded dramatically different estimates of standing stock of OC in our study area of 223 km²: 80,901, 58,406, 16,437 and 6,475 t of OC, respectively. Our study demonstrates that high-resolution mapping is critically important for improved estimates of OC stocks on continental shelves, and to the identification of carbon hotspots that need to be considered in seabed management and climate mitigation strategies.

1 Introduction

30 1.1 Blue Carbon

Blue Carbon has received tremendous interest as a natural option for climate change mitigation due to the fact that some marine habitats can store disproportionate amounts of organic carbon (OC) on an area-by-area basis compared to terrestrial habitats (Hilmi *et al.*, 2021). The Intergovernmental Panel on Climate Change (IPCC) defines Blue Carbon as: “*All biologically driven carbon fluxes and storage in marine systems that are amenable to management*” (2019). By this definition, Blue Carbon is therefore associated with vegetation in coastal zones,

35

such as tidal marshes, mangroves, and seagrasses (McLeod *et al.*, 2011). OC in marine sediments are often not included in Blue Carbon calculations and definitions since these environments do not sequester carbon via photosynthesis (Lovelock *et al.*, 2019). However, marine sediments are essential carbon reservoirs and regulate climate change by effectively burying OC over thousands to millions of years if left undisturbed (Berner, 2003; 40 Burdige, 2007). Studies are therefore beginning to acknowledge marine sediments as an emerging Blue Carbon ecosystem (Howard *et al.*, 2023).

The fate and flux of organic carbon in benthic systems is influenced by a range of factors acting over different timescales (Middelburg, 2018), including natural and anthropogenic-induced processes (Bianchi *et al.*, 2021, 2023). Recent studies have concluded that, on a global scale, all bottom trawling and dredging disturbs the seafloor 45 with an estimated 1.47 Pg of aqueous CO₂ emissions (Sala *et al.*, 2021). However, these estimates have substantial errors (Epstein *et al.*, 2022) and often ignore that the mineralization of benthic carbon stores comes from natural cycles (Hilborn *et al.*, 2023). Combined, these studies emphasize that further understanding of sediment ocean carbon processes are urgently required to determine if bottom trawling and dredging could cause the semi-permanent OC stocks in surficial marine sediments to remineralize back to CO₂ (Bianchi *et al.*, 2023). Also, future 50 studies into new approaches to determining the distribution of OC are essential to locate areas of carbon-rich seabed. Furthermore, this research could expand the definition of Marine Protected Areas (MPAs) to include areas of high OC stock (Oceans North, 2024).

1.2 Seafloor Substrate

Sediment characteristics, such as mud content, are known to influence the distribution of OC in marine ecosystem 55 (Burdige, 2007; Serrano *et al.*, 2016), with recent studies highlighting the importance of sediment properties as predictors of organic carbon storage in Blue Carbon ecosystems (Dahl *et al.*, 2016; Krause *et al.*, 2022). In shelf environments, where sediment heterogeneity can be high, sediment classification maps may therefore offer a mechanism to determine areas of low and high OC content (Bianchi *et al.*, 2021). Multibeam-echosounder (MBES) systems provide information about the environmental characteristics of the seafloor, such as depth, 60 substrate hardness, and sediment characteristics, by collecting bathymetry and backscatter information, which can be used to determine seafloor morphology and as a proxy for seafloor substrate type (Brown *et al.*, 2011). Advancements in MBES have allowed us to create spatially continuous high-resolution maps of the ocean floor (Brown *et al.*, 2011; Buhl-Mortensen *et al.*, 2021; Misiuk and Brown, 2024), at horizontal resolutions down to sub-meter scales (depending on water depth and sonar specifications; Mayer *et al.*, 2018). Seafloor sediment 65 mapping describes the use of geophysical and physical sampling systems to determine the character of the surface sediments, and includes mapping quantities of clay/silt, sand, gravel, cobble, and boulder using the Wentworth scale (e.g., Misiuk *et al.*, 2019). Recent methods for producing seabed sediment maps combine high-resolution MBES with ground-truth sampling data using machine learning algorithms (Misiuk *et al.*, 2019). Statistical techniques include k-Nearest Neighbour (Lucieer *et al.*, 2013; Stephens and Diesing, 2014), Artificial Neural 70 Networks (Huang *et al.*, 2012; Stephens and Diesing, 2014), and Bayesian Decision Rules (Simons and Snellen,

2009; Stephens and Diesing, 2014). The most widely used statistical model for substrate classification and regression maps is Random Forest, due to its ease of implementation and a robust capacity for handling complex, non-linear relationships between environmental variables and ground truthing while avoiding overfitting (Stephens and Diesing, 2015; Misiuk and Brown, 2024).

75 **1.3 Benthic Carbon Mapping**

Early marine carbon mapping studies have applied interpolation methods comprising semi-variogram analyses and kriging to spatially predict OC in surficial sediments (Mollenhauer *et al.*, 2004; Acharya and Panigrahi, 2016). More recently, soil OC has been modeled using multiple methods in terrestrial ecosystems. Mallik *et al.* (2022) compared artificial neural networks (ANN), Empirical Bayesian Regression Kriging (EBRK), and hybrid
80 approaches combining the two, including ANN-OK (ordinary kriging) and ANN-CK (cokriging). They found that the EBRK method outperformed all other models with highest values of R^2 (0.936) (Mallik *et al.*, 2022). The EBRK method has been widely used in terrestrial soil carbon models but has still not been explored for marine sediment carbon models. More recent studies have utilized machine learning algorithms to model and map OC at broad spatial scales at the seafloor (Atwood *et al.*, 2020; Diesing *et al.*, 2017; Smeaton *et al.*, 2019). Diesing *et al.*
85 (2017) used Random Forest to model particulate OC (POC) at the seafloor using measurements from physical seafloor samples, and spatially continuous seafloor environmental variables (500 m grid resolution) covering the Northwest European continental shelf. Similarly, Smeaton *et al.* (2019) generated a map of seafloor substrate using the Folk classification and calculated the OC stock per substrate class (100 m grid resolution). This latter study was the only one amongst those listed to utilize MBES data to predict OC stock. Epstein *et al.* (2024) also applied
90 Random Forest to model OC stocks and accumulation rates in surficial sediments of the Canadian continental margin at a coarse resolution (200 m grid resolution) and emphasize that ignoring the geographic extent of hard substrate (i.e., bedrock) at such broad spatial scales could inflate carbon stock estimates. These studies have been critical to understanding the carbon hotspots at broad spatial scales, as the traditional lower-resolution maps often lead to oversimplification and inconsistency in carbon averaging. However, understanding distributions of
95 sedimentary OC at a higher spatial resolutions may be required for effective seabed management strategies (Legge *et al.*, 2020).

High-resolution maps of OC have been produced at a local scale using 48 m resolution backscatter from MBES surveys as a predictor (Hunt *et al.*, 2020, 2021). Backscatter can be predictive of seabed sediment properties and was hypothesized to be a proxy for OC based on observed empirical relationships between grain size and OC, and
100 also potentially other additional sedimentary properties that influence backscatter reflectance (Hunt *et al.*, 2020). Backscatter data may thus be valuable where sediment data are scarce. Hunt *et al.* (2020) indicated that backscatter reliably captured information regarding the spatial heterogeneity of the seabed, and that OC correlated strongly with the MBES backscatter signal as a function of sediment composition. However, a more recent study suggested that backscatter distinguishes between coarse and fine sediments (low and high OC) but struggled to differentiate
105 fine-scale variability within finer-grained sediments (Hunt *et al.*, 2021). Differences in results between these

studies could be due to the different geographical setting of the studies, limited and asynchronous data, sediment mobility over time, or complex environmental processing of OC in shelf sediments (Hunt *et al.*, 2021).

The studies in the North-West European continental margin (Diesing *et al.*, 2017, 2021; Hunt *et al.*, 2020; Hunt *et al.*, 2021; Legge *et al.*, 2020; Smeaton *et al.*, 2021) have shown promising early results. Other studies of carbon stocks have been conducted in the North American coastal region but without spatially explicit estimates (Fennel *et al.*, 2019; Najjar *et al.*, 2018). Overall, spatially mapping OC at the seabed has only been attempted at a few locations globally, and there is an urgent need to establish robust approaches to obtaining spatial estimates of OC at the seafloor. High resolution OC mapping may additionally help to improve current estimates of seafloor OC stocks and provide insight on marine sediments as an emerging Blue Carbon ecosystem. As a conservation Area of Interest (AOI) for the Canadian government, the Eastern Shore Islands (ESI) is an ideal location to test emergent OC mapping methods; it comprises a heterogeneous seabed that may provide insight on the effectiveness of various baseline sediment OC estimation and mapping methodologies.

This study addresses three key questions:

1. What is the spatial distribution of seafloor sediment types in the ESI area?
2. Are seafloor sediments a good high-resolution proxy that enable accurate estimation of OC stock?
3. Does the spatial heterogeneity of substrate type and carbon content influence estimates of OC stock?

2 Study Area

The study region is located within the ESI, approximately 60 km northeast of Halifax (Nova Scotia, Canada, Figure 1). The site stretches from Lower West Jeddore to Fern Hill and extends approximately 25 km from the mainland with an area of approximately 223 km² (Fisheries and Oceans Canada, 2019) (Figure 1). The ESI is a conservation AOI for the Canadian government due to its unique coastal habitat and significant quantities of kelp beds and eelgrass. The estuaries and rivers that drain into the site are considered important habitats for endangered species like Atlantic salmon and juvenile Atlantic cod. Furthermore, the hundreds of islands have been identified as an Ecologically and Biologically Significant Area (EBSA), which provides essential nesting and foraging ground for many colonial seabirds and shorebirds, including purple sandpiper, and roseate tern which are endangered according to the Species at Risk Act (Fisheries and Oceans Canada, 2019).

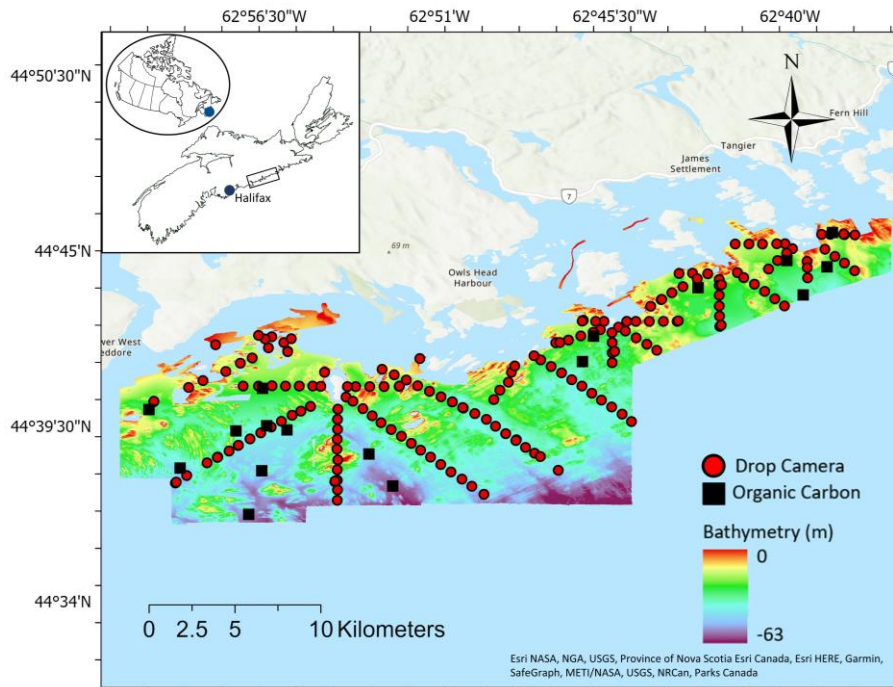


Figure 1. Seafloor MBES bathymetry and sample locations for the survey area at the Eastern Shore Islands, Nova Scotia, Canada (inset).

135 The study area has a water depth between 31 and 63 m. The surficial geology of the ESI is spatially heterogeneous, with bedrock overlaid by mud, sand, gravel, cobble, and boulder substrates (King, 2018). The bedrock topography is an extension of the terrestrial geomorphology and heavily influences the type and distribution of the surficial deposits. The glacial imprint is substantial in the area, having deposited a sequence of till and glaciomarine mud, which lie directly on the bedrock (King, 2018). There is also a thin layer of wave-modified sand and gravel, and

140 more recent deposits of estuarine mud derived from coastal erosion (Fisheries and Oceans Canada, 2019). Ocean surface temperatures in the ESI are around 1° C in winter for the 0–100 m depth range and increase in the summer with some stratification leading to surface temperatures exceeding 15° C (Fisheries and Oceans Canada, 2019). By the fall, mixing deepens this warm layer. Ocean currents run predominantly southwestwards, with some fluctuation around the coast (Feng *et al.*, 2022). The combination of upwelling, currents, and wind allows for the

145 mixing of nutrients, acting as an essential component of the marine food web in the region (Fisheries and Oceans Canada, 2019). Nutrients are derived from river, coastal runoff and mixing. They are depleted in the spring due to phytoplankton blooms and replenished in the fall when upwelling is predominant (Fisheries and Oceans Canada, 2019). Major human activities in this area include lobster fishing, recreational fishing, and boating, but the human impact is low due to low population density and reduced coastal development compared to nearby Halifax and St.

150 Margarets Bay (Fisheries and Oceans Canada, 2019).

3 Materials and Methods

To quantify OC stock in the ESI, sediment samples were collected, and OC content and sediment grain size were measured. OC density was calculated for each sample, and four OC stock estimations were generated. The first assumed a homogenous seafloor by scaling up the average OC density to the entire study area. The second also assumed a homogeneous seafloor but used Empirical Bayesian Kriging (EBK) to derive the spatial variability of OC density for the study area. Both scenario 1 and 2 were conducted to evaluate OC estimates when no high-resolution mapping data is available. To further refine the OC stock estimates, a substrate classification map was developed by combining high-resolution seafloor predictor variables (derived from multibeam sonar data – see below) and subsea camera imagery of the seabed. The substrate classification map partitioned the study area into hard and soft substrates. The third OC stock estimate utilized the sediment classification and scaled the average OC density to the area of the soft substrate. The final OC stock estimate also utilized the sediment classification map but used Empirical Bayesian Regression Kriging (EBRK) prediction to incorporate the spatial variability of the OC density within the soft substrate only. Scenarios 3 and 4 determine OC estimates when sediment information and high-resolution mapping data is available. An overview of the analysis workflow is shown in Figure 2.

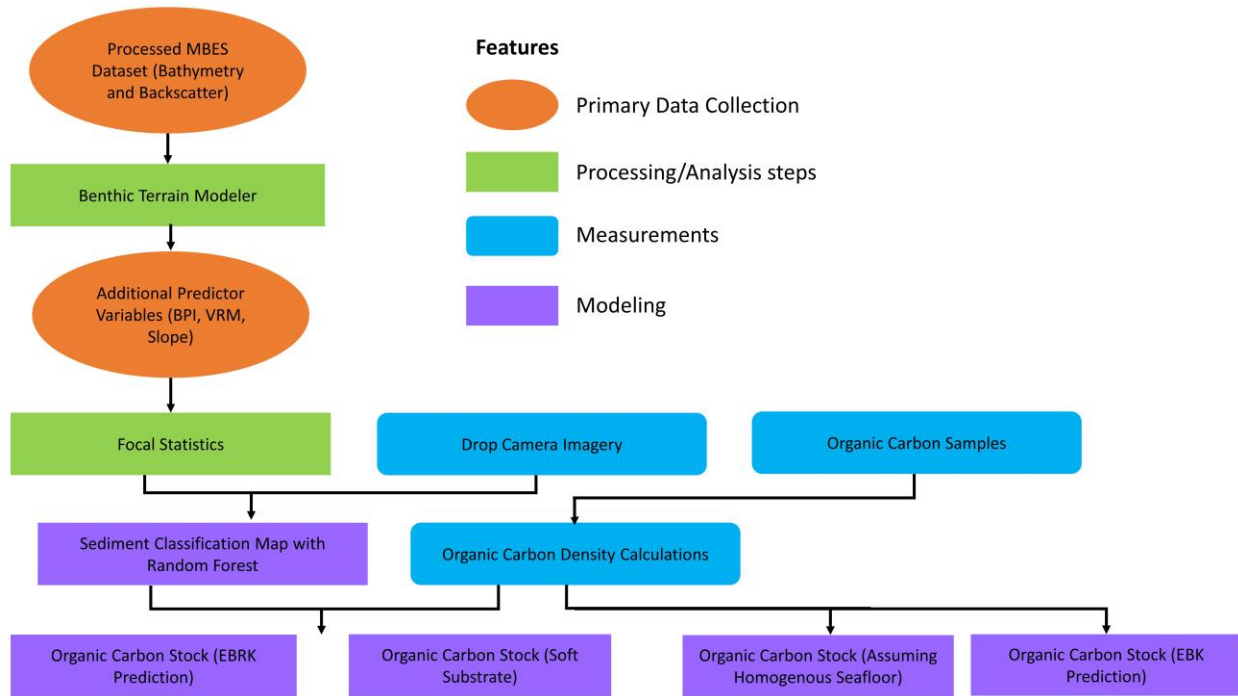


Figure 2. General analysis steps used to estimate organic carbon for four scenarios.

3.1 Hydrographic Datasets

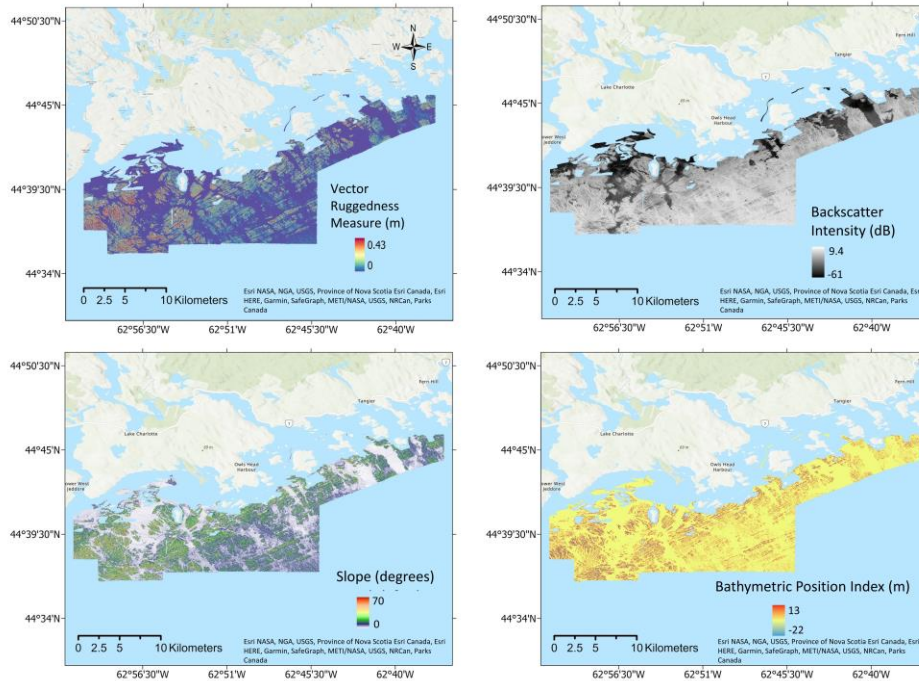
MBES data were collected by the Canadian Hydrographic Service over two separate surveys (20 June – 29 July 2019; 17 August – 05 September 2020) (Bondt, 2019, 2020). Three launches were used to complete this survey –

the *CSL Kestrel*, *CSL Tern* and *CSL Pelican*. The survey launch *CSL Kestrel* was equipped with an R2Sonic 2022 multibeam echosounder. The survey launches *CLS Tern* and *CSL Pelican* were outfitted with Kongsberg EM2040C and EM2040C Dual Head echo sounders, respectively. All surveys were conducted at MBES operating frequencies of 200-400kHz. Vessel position and orientation were corrected in real time by Trimble/Applanix POSMV V5 motion compensation systems. Echosounder data was corrected for sound velocity in real time using Applied Microsystems Limited sound velocity sensors. The vessel position was recorded in real-time using the CANNET RTK NTRIP connected directly through the POSMV. Raw position and orientation data from the POSMV were logged throughout the survey for further post-processing where required. Bathymetry and backscatter data were processed using the QPS software suite. Bathymetry data were processed in Qimera 2.5.3 to generate a bathymetric digital elevation model (DEM) for the survey area. Backscatter data were processed in FMGT 7.10.2 to generate backscatter mosaics for each of the data sets. Backscatter data were not calibrated; the different survey data sets were harmonised using bulk shift methods (Misiuk *et al.*, 2020, 2021; Haar *et al.*, 2023) from areas of overlap between the survey data sets to generate a corrected backscatter mosaic for the entire study area.

Seafloor morphology features were derived from the primary bathymetric datasets to provide additional predictor variables for sediment classification modelling. These were selected based on literature review, expert suggestions, and access to data, and were calculated using ArcGIS Pro 3.1.2 using the Benthic Terrain Modeler (BTM) 3.0 Toolbox. The terrain features included slope, bathymetric position index (BPI) and vector ruggedness measure (VRM), which are considered useful predictors for seabed substrate classification (Stephens and Diesing, 2015; Misiuk *et al.*, 2019) (Table 1) (Figure 3). The Focal Statistics tool was used to obtain the mean value for each predictor variable over a 20 by 20 pixel neighbourhood to reduce noise. The variables were then used in both the substrate map and the OC model.

Table 1. Description of predictor variables used to model sediment type.

Environmental Variables	Description	Resolution	Units
Bathymetry	Depth of the seafloor	2 m	meters
Backscatter	Measure of intensity of acoustic signal from MBES and indicator of bottom hardness	2 m	relative dB
Slope	Measures maximum change in elevation (steepness)	2 m	degrees
Vector Ruggedness Measure (VRM)	Measures terrain ruggedness of grid cells within a neighbourhood	2 m	meters
Bathymetric Position Index (BPI)	Differences in values of centre cell to mean of surrounding cells.	2 m	meters



195

Figure 3. Backscatter, Slope, VRM and BPI data mapped in the Eastern Shore Islands study area.

3.2 Seabed Sediment Sampling

Sampling surveys for OC and grain size were conducted between 9 - 27 May 2022 from the *MV Island Venture*. Sampling locations were randomly placed in regions of low MBES backscatter, which indicate softer, unconsolidated sediments where grab sampling should be successful (Figure 3). Acoustic backscatter was used to select sampling locations as a proxy for sediment grain size (Goff *et al.*, 2000; Sutherland *et al.*, 2007; Collier *et al.*, 2014; Hunt *et al.*, 2020). A 0.1 m² Van Veen grab fitted with a GoPro camera was operated to collect sediment samples and drop camera imagery at each sample location, with the grab penetrating up to ~10 cm depth into the substrate. The GPS position of the research vessel was recorded at the point of contact at the seabed at each grab station. A total of 17 grabs were successful in areas of soft substrate. Generally, it is difficult to sample a coarser sediment matrix successfully, and these sediment types are often under-represented in sedimentary carbon studies (Hunt *et al.*, 2020). After thoroughly mixing the sediment in the Van Veen grab, 0.907 kg (32 oz) subsamples of sediment were taken from the grabs, and each placed in a plastic container for OC analysis. Following collection, these samples were stored in a cooler during the day and put into a freezer in the evening.

3.3 Processing of Sediment Grab Samples

Prior to sediment grain size and OC analysis, the samples were dried from frozen in the oven at 60°C overnight and kept in a dark dry cabinet. Sedimentary OC from the grab samples was quantified using an elemental analyzer (EA, Elementar Microcube) with a detection limit of 0.03 mg. Based on the method of Verardo *et al.* (1990), a section of the grab samples (5 g) was ground using a mortar and pestle to form a homogenous powder. Two samples (ES-31, ES-35) contained significant concentrations of sediment grains coarser than 2 mm (around 30%

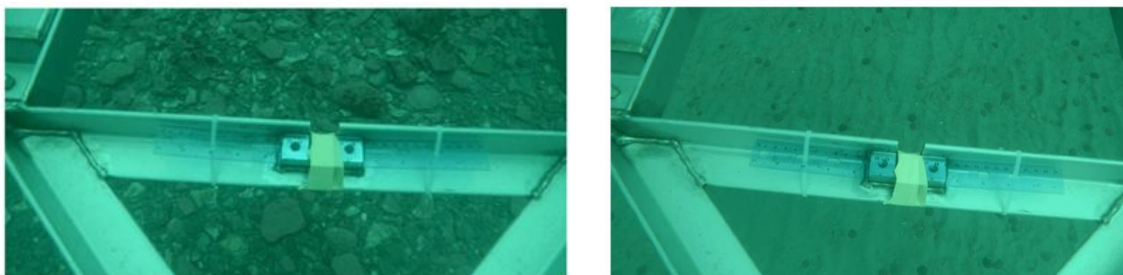
of sample). These sand grains were removed using mesh sieves prior to grinding and EA analysis, but final sedimentary OC concentrations were adjusted to total sample weight following EA analysis. Silver capsules were used to weigh the initial mass (0.5-0.7 mg), and acid fumigation was performed by exposing the samples to 37% hydrochloric acid (HCl) to remove any inorganic carbon. These capsules were then placed in an oven overnight at 60°C before analysis.

The remaining section of the grab samples was used for sediment grain size analysis, following the protocol of Mason (2011). The sediment was first split into pebble/cobble (>4000 µm), gravel (>2000 µm) and fine sediment (<2000 µm) material using mesh sieves. The fraction <2000 µm was evaluated using a Beckman Coulter LS 13 320 particle size analyzer at the Bedford Institute of Oceanography. Following the guidance of Mason (2011), the samples were not treated with acid or hydrogen peroxide because the samples had relatively low organic content. The results from the coarse and fine-scale fractions were combined into a full particle size distribution to determine the percentage of mass of the total for each sample (supplementary material). It should be noted that dry bulk density was not measured directly in this study but was instead calculated (see section 3.6).

3.4 Subsea Video Surveys

A total of 174 drop camera videos were collected by Fisheries and Oceans Canada (DFO) over 13 days during September and October 2017 aboard the vessel *RV Sigma-T* (Fisheries and Oceans Canada *et al.*, 2019). (Figure 1). A HD subsea video camera (SV-HD SDI) was used with camera time and position recorded using a video overlay streamed from the chart plotter (Vandermeulen, 2018). The video feed with overlay outputted to a direct-to-disk HD recorder and a standard low-power LED TV. The GPS antenna for the navigation system was mounted on the roof of the wheelhouse approximately 10 m from the drop camera when deployed off the stern gallows. In this manner, all positional information in the video overlay was offset by ~10 m and was adjusted during post-processing. Approximately three minutes of moving video was recorded at each drop camera location. The centre of each video drift was recorded as the station location. All the drop camera sites occurred at depths > 10 m. The GoPro camera imagery collected with the grab sampler during OC sampling in 2022 (see sediment sampling section above) was additionally incorporated with the drop camera imagery for subsequent analysis (Figure 1).

From each video station, a presence (1) and absence (0) of different sediment types were recorded in post processing. The data was classified into two sediment types: hard substrate (rock, boulder, cobbles, pebbles, and gravel), and soft substrate (mud and sand) (Figure 4) (supplementary material).



250 **Figure 4. Example of seafloor imagery from each of the two substrate classes: hard Substrate (left); soft substrate (right). Photos from a GoPro camera mounted on the Van Veen grab. Width of images are approximately 0.5 m, with the frame of the grab providing scale for classification of substrata.**

3.5 Sediment Classification Model

Random Forest has been used in previous carbon mapping studies due to its high predictive accuracy, capacity to manage many predictor variables, and unbiased internal validation (Diesing *et al.*, 2017). In our study, Random Forest was used to model the sediment grain size class to inform OC content estimation using R version 4.3.1 with the randomForest package (Liaw and Wiener, 2002). The model was initially trained with default hyperparameters ($n_{tree} = 500$, $m_{try} = 2$, $nodesize = 1$) using the substrate classification observations and all predictor variables (bathymetry, backscatter, BPI, VRM and slope). Random Forest is an ensemble modelling approach comprising many individual classification trees, each grown on a bootstrapped version of the dataset. The observations not selected for a given tree are termed the “out-of-bag” (OOB) observations. Given enough trees, each response observation will be represented in the OOB sample multiple times. By predicting the OOB values for each individual tree during model training, the results can be aggregated over all trees to provide a useful set of validation predictions that were not used to inform training. The OOB observations were used here to estimate predictor variable importance by permuting the predictor values and measuring the resulting increase in OOB error (Liaw and Wiener, 2002). Random Forest is generally considered robust to the use of correlated predictors and estimates of importance additionally suggested contribution to the model by all variables, which were thus retained. Informal trials suggested that a model of 100 trees (i.e., $n_{tree} = 100$) provided sufficient predictive capacity but improved computational speed. After training the final model with these parameters, a confusion matrix was generated using the OOB observations and predictions to evaluate the map accuracy, and the model was then predicted across the full map extent using the predictor variable rasters. The kappa statistic was used to evaluate the model predictions, indicating how well predictions agree with observations beyond the level of agreement that could be expected by chance:

$$k = \frac{p_o - p_e}{1 - p_e} \quad (1)$$

275 where κ is the value of kappa between -1 and 1 , p_o is the proportion correctly classified and p_e is the proportion correctly classified due to chance, based on the frequency of observations and predictions of each class. A kappa score of 0 is considered “poor” agreement, while values in the range 0 to 0.20 are often considered “slight” agreement, 0.21 to 0.40 as “fair”, 0.41 to 0.60 as “moderate”, 0.61 to 0.80 as “substantial” agreement, and 0.81 to 0.99 as “almost perfect” agreement.

280 3.6 Estimation of Standing Stock of Organic Carbon

The elemental analyser reports OC value as a proportion (weight %). Dry bulk density was not measured directly in this study but calculated from estimated porosity and density. Porosity (Φ) was calculated from predicted mud content (dimensionless fraction), which is a combination of clay and silt from the grain size distribution measurements using the equation (2) derived from Jenkins (2005).

$$285 \quad \Phi = 0.3805 * C_{mud} + 0.42071, \quad (2)$$

where Φ and C_{mud} (mud content) are dimensionless fractions. The equation was derived based on data from the Mississippi-Alabama-Florida shelf, and it is assumed that the equation is not site-specific (Diesing *et al.*, 2017).

Dry bulk density (p_d) of the sediment was estimated using the porosity and sand grain density ($p_s = 2650 \text{ kg m}^{-3}$) (Diesing *et al.*, 2017; Hunt *et al.*, 2020):

$$290 \quad p_d = (1 - \Phi) p_s \quad (3)$$

The organic carbon density (kg m^{-3}) was calculated by multiplying the %OC (Y) (expressed as a decimal proportion) by the sediment dry bulk density (p_d). Following prior studies that quantified marine sedimentary OC (e.g., Diesing 2017, Hunt 2021), the standing stock of organic carbon per grid cell (m_{oc}) was estimated by multiplying the average OC density by the sampling depth of the Van Veen grab ($d = 0.1 \text{ m}$), area of mapped grid cell ($A = 4 \text{ m}^2$) and converted to metric tonnes (divided by 1000) using the equation (4) below:

$$295 \quad m_{oc} = (Y * p_d * d * A) / 1000 \quad (4)$$

Finally, the total standing stock was the m_{oc} multiplied by the total pixels in the study site (scenarios 1 and 2) or the total pixels in the soft substrate (scenarios 3 and 4).

3.7 Spatial Interpolation of Organic Carbon – No Substrate

300 After the m_{oc} was calculated for each sample, EBK was used to spatially interpolate m_{oc} within the entire study site. EBK is a geostatistical interpolation method that builds a kriging model by subsetting the study area, coupled with multiple simulations to obtain the best fit (Krivoruchko and Gribov, 2019). This process finally creates several simulated semi-variograms, each of which is an estimate of the true semi-variogram for the subset (Pellicone *et al.*, 2018). EBK differs from other kriging methods since it considers the uncertainty in the semi-variogram estimation step, providing an estimate of the prediction standard errors. An exponential semi-variogram and an empirical transformation were selected and EBK was executed in the geostatistical wizard in ESRI ArcGIS Pro 3.1.

3.8 Spatial Interpolation of Organic Carbon Density – Soft Substrate

310 EBRK was used for the spatial interpolation of OC density and estimation of values at unknown locations within the extent of the soft substrate. EBRK is a geostatistical interpolation method that combines ordinary least square regression and kriging to provide accurate predictions of non-stationary data at a local scale (Giustini *et al.*, 2019).

An exponential semi-variogram model and an empirical transformation were selected for the EBRK model, which was evaluated using leave-one-out cross-validation (Mallik *et al.*, 2022). The EBRK method is different from EBK in that predictor variable information is accommodated by including their principal components as regression variables prior to the kriging step. Thus, all the predictor variables from the substrate classification map (bathymetry, backscatter, bpi, vrm and slope) were masked to the soft substrate area in ESRI ArcGIS Pro 3.1 and included in the EBRK model to improve estimation of OC density.

3.9 Cross Validation Methods

To estimate the accuracy of the EBK and EBRK predictions, the mean error (ME) and the root-mean-square error (RMSE) were calculated. ME is the average of the cross-validation errors, measures model bias and should have a value close to zero (Acharya and Panigrahi, 2016).

$$ME = \frac{1}{n} \sum_{i=1}^n \{z(xi) - \hat{z}(xi)\} \quad (5)$$

RMSE measures the difference between the predicted and the observed values and estimates the standard deviation of the residuals (Boumpoulis *et al.*, 2023). A small root mean square error (RMSE) indicates that the model has performed well and can predict the data accurately.

$$RMSE = \left[\frac{1}{n} \sum_{i=1}^n \{z(xi) - \hat{z}(xi)\}^2 \right]^{1/2} \quad (6)$$

The $z(xi)$ is the observed OC and $\hat{z}(xi)$ is the prediction of OC at location xi , and n is the number of observations. These cross-validation error parameters were calculated within the Geostatistical Wizard Tool in the ESRI ArcGIS Pro 3.1.

4 Results

4.1 Grain size Distributions, Sediment Properties, and Organic Carbon Content

Van Veen grab samples provided grain size and OC measurements at each station (Table 2). It is important to note that silt and clay were merged into a single mud class to estimate the OC stock (Burdige, 2007; Hedges and Keil, 1995).

Table 2. Raw data from grab samples including grain size and OC measurements.

Station	>4000 um (%)	>2000 um (%)	Sand Content (%)	Silt Content (%)	Clay Content (%)	Porosity	Dry Bulk Density (kg/m ³)	Organic Carbon Content (%)
ES-02	0.27	0.08	54.3	38.4	7.13	0.59	1077.6	1.22

ES-03	0.003	0.06	90.8	7.11	2.03	0.46	1443.0	0.12
ES-04	0.33	0.01	93.7	4.28	1.69	0.44	1475.1	0.13
ES-07	0.00	0.00	24.4	65.2	10.3	0.71	773.0	1.85
ES-15	0.59	0.11	94.6	3.44	1.29	0.44	1487.4	0.06
ES-17	2.07	0.30	63.7	30.5	4.18	0.55	1185.1	0.10
ES-18	0.60	0.04	80.2	17.4	1.93	0.49	1340.5	0.23
ES-19	0.00	0.04	96.7	2.15	1.12	0.43	1502.2	0.08
ES-21	0.14	0.10	91.4	7.23	1.17	0.45	1450.4	0.06
ES-23	0.08	0.21	93.8	4.68	1.27	0.44	1475.1	0.07
ES-25	0.006	0.01	95.4	3.50	1.05	0.44	1489.3	0.05
ES-27	0.04	0.05	85.0	13.3	1.67	0.48	1384.7	0.07
ES-28	0.00	0.05	85.2	13.2	1.63	0.48	1385.8	0.08
ES-29	0.00	0.02	86.7	11.4	1.87	0.48	1401.4	0.08
ES-31	21.42	9.97	45.8	22.2	1.11	0.51	1199.2	0.57
ES-34	2.15	0.71	52.4	39.9	6.15	0.59	1071.1	0.61
ES-35	34.00	0.37	17.3	44.0	4.26	0.61	793.01	0.62

4.2 Relationship between Grain Size and Organic Carbon

340 A linear regression was performed to examine the relationship between OC content (%) and the percentage grain size composition of mud. There was a significant positive relationship between OC content and percent mud ($p < 0.001$; $R^2 = 0.81$) (Figure 5), suggesting that % mud content may be useful as a proxy for OC content, as also observed at many other sites (Burdige, 2007; Hedges and Keil, 1995; Hunt *et al.*, 2021).

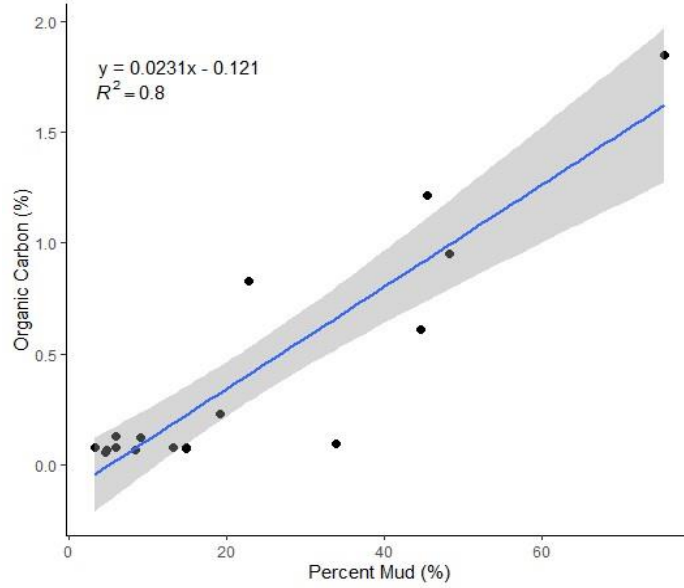
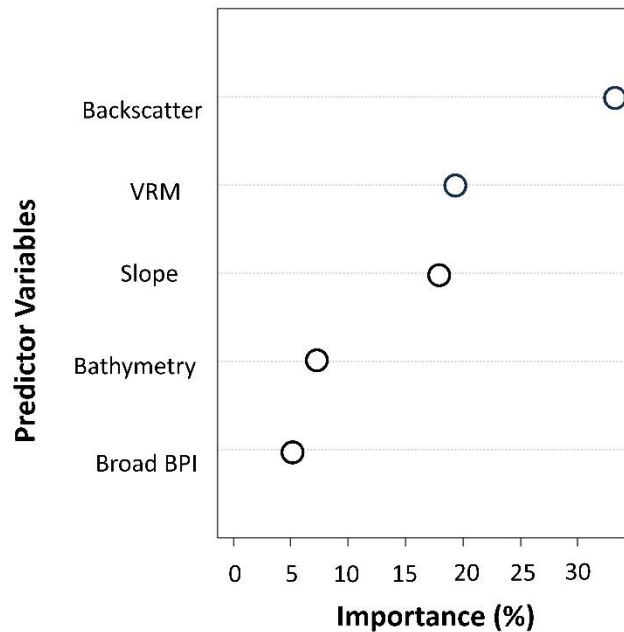


Figure 5. Linear regression indicating the relationship between OC and percent mud. The grey area represents a 95 percent confidence interval for the slope of the regression line.

345 4.3 Substrate Classification Map

Outputs from Random Forest indicated that bathymetry, backscatter, vector ruggedness measure (VRM) and slope were all important for the sediment classification. Figure 6 shows the relative importance of the five variables in the model. Backscatter was the most important variable for predicting sediment type, followed by VRM, slope, bathymetry, and BPI.



350

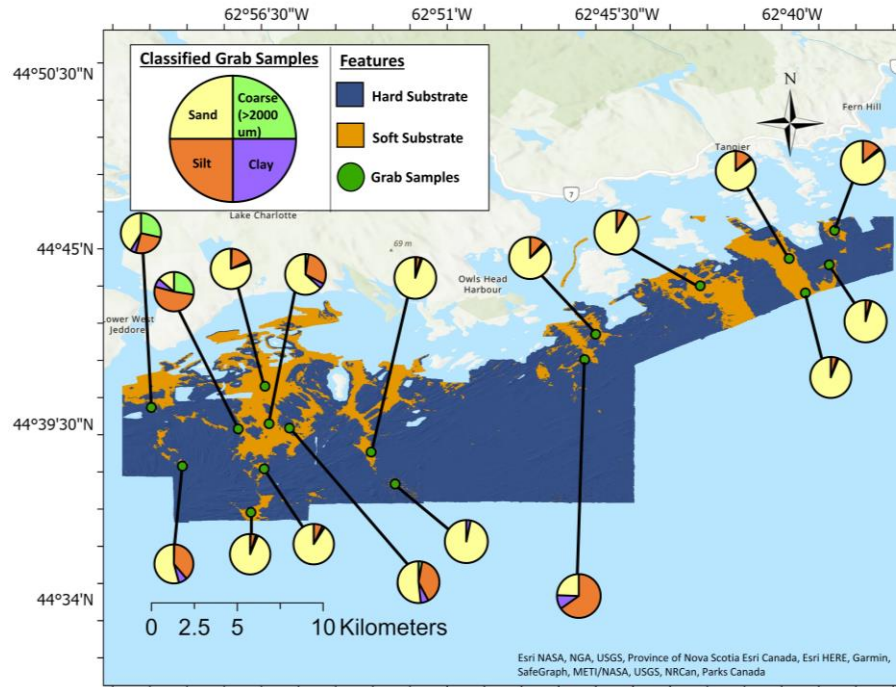
Figure 6. The importance of predictor variables as estimated using Random Forest.

The confusion matrix calculated using the OOB observations is presented in Table 3. A kappa score of 0.69 indicates substantial agreement between observations and predictions of each class, suggesting that the model was able to successfully differentiate soft and hard substrates within the study area.

355 **Table 3. Confusion matrix of substrate type predictions.**

		Observed	
		Hard Substrate	Soft Substrate
Predicted	Hard Substrate	129	16
	Soft Substrate	9	44

360 The sediment classification map revealed that the hard substrate was the most spatially extensive (178 km²) whereas the soft substrate class was smaller, covering approximately 45 km² of the study area, corresponding with contiguous patches of relatively low relief seafloor (Figure 8). Sediment grain size from the grab samples revealed grain size percentiles d₁₀=17 um, d₅₀= 147 um and d₉₀= 1822 um. This suggests predominantly sandy sediments, with varying smaller proportions of silt and clay (Figure 7). Two samples were comprised of around 30% coarse substrate (>2000 um) (Figure 7).



365 **Figure 7. Sediment classification map indicating predicted soft (orange) and hard (blue) substrates. Pie charts depict ratios of sand (yellow), silt (orange red), clay (purple), and coarse (green) for each sediment sample collected.**

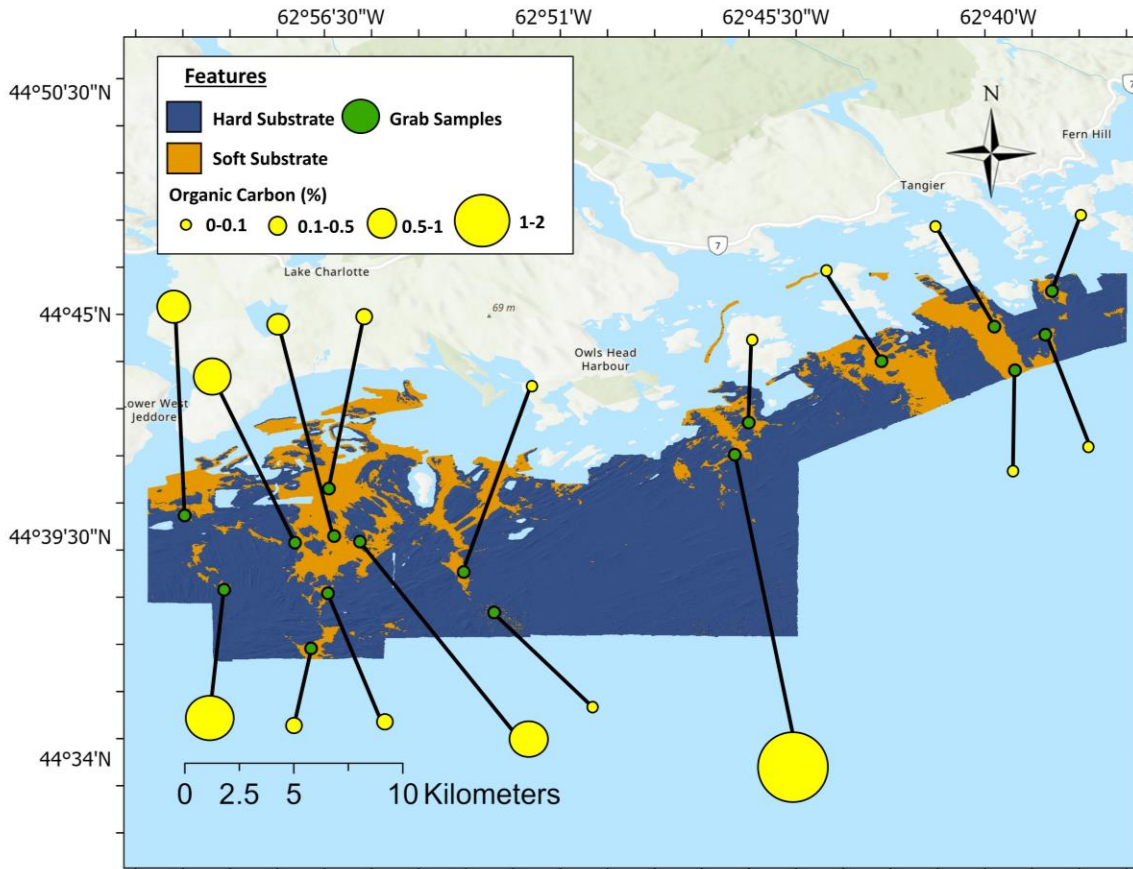


Figure 8. Sediment classification map indicating areas of soft (orange) and hard (blue) substrate. Proportional symbols of OC indicate the sampled percentage (yellow).
370

4.4 Organic Carbon Density Maps

Predicted OC density was high on the west part of the study site near lower west Jeddore and in the middle of the study area near Owls Head Harbour (Figure 9). Cross-validation of the EBK model indicated the accuracy of the OC density predictions were $ME=-0.27 \text{ kg/m}^3$, and $RMSE=4.21 \text{ kg/m}^3$, suggesting low bias but also that the magnitude of prediction error was substantial compared to the range of the observed data (e.g., Figure 9).
375

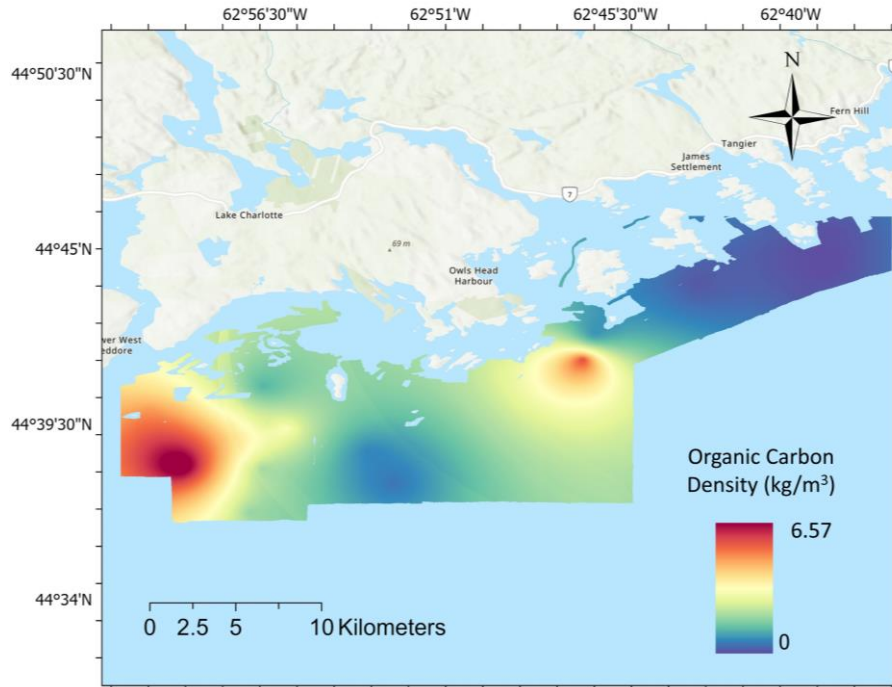


Figure 9. Spatial interpolation of OC using EBK.

The EBRK model prediction suggested high OC density in the west and south-west of the study area. A significant quantity of OC density was predicted eastward near Owls Head Harbour (Figure 10). The lowest OC density was predicted at the eastern part of the study area with quantities close to zero. Cross-validation indicated $ME = -0.31 \text{ kg/m}^3$ and $RMSE = 3.52 \text{ kg/m}^3$, suggesting slightly higher bias than the EBK model, yet more accurate predictions.

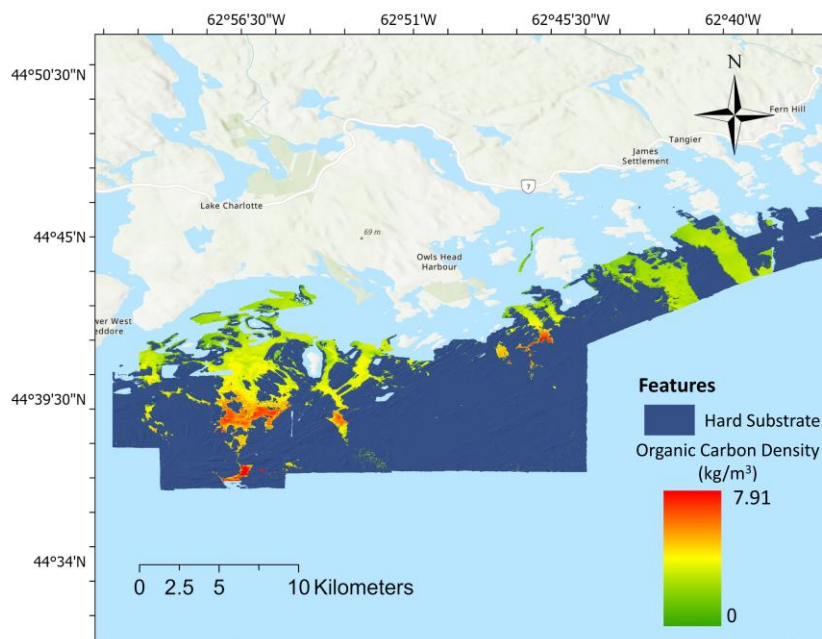


Figure 10. Spatial interpolation of OC using EBRK.

385 **Table 5. Outputs from the EBRK model predicting OC density within the soft substrate. Model performance results are given by the ME= Mean error and RMSE= Root Mean Squared Error.**

No of simulation	Model selected	No of variables	ME	RMSE
100	Exponential	5	-0.31	3.52

4.5 Organic Carbon Estimates

Estimates of average OC density, OC stock per pixel and total OC stock were calculated for all four scenarios (Table 6).

390 **Table 6. Calculations used to determine the total stock of OC in the mud/sand sediment type and the total stock of OC in the entire study area.**

Maps	Average density of OC per grid cell (kg/m ³)	Average OC stock per grid cell (kg per m ²)	Total grid cells	Total stock of OC in study area (t)
Scenario 1: assuming homogenous seabed (entire study site)	3.62 (0.804 to 14.31)	1.45 (0.322 to 5.72)	5.58E+07	80,901 (17,949 to 319,335)
Scenario 2: EBK method (entire study site)	2.62 (1.08 to 6.57)	1.05 (0.432 to 2.63)		58,406 (24,092 to 146,560)
Scenario 3: assuming heterogenous seabed (soft substrate)	3.62 (0.804 to 14.31)	1.45 (0.322 to 5.72)	1.13E+07	16,437 (3,647 to 68,882)
Scenario 4: EBRK method (soft substrate) OC	1.45 (0 to 7.91)	0.57 (0 to 3.16)		6,475 (0 to 35,850)

395

5 Discussion

400 Our study explores how high-resolution spatial models can improve carbon budget estimates. We have described a quantitative spatial model of hard and soft substrate in a continental shelf environment and determined four estimates of OC stock in the surficial sediments (top 10 cm): scaling to the entire study area (scenario 1), interpolating OC density using an EBK model (scenario 2), scaling to only the soft substrate (scenario 3), and refining m_{oc} within the soft substrate estimated from an EBRK model (scenario 4). The results demonstrate that
405 as spatial models become more detailed, the OC stock estimation increases in accuracy but decreases the overall predicted OC stock.

5.1 Evaluation of Sediment Map

The sediment map effectively classified the hard and soft substrate ($\kappa=0.69$) and significantly refined our understanding of the detailed distribution of the OC. Previous studies have applied similar machine learning
410 modelling approaches with success (Stephens and Diesing *et al.*, 2015; Misiuk *et al.*, 2019; Mitchell *et al.*, 2019; Epstein *et al.* 2023). Our results further demonstrate that this approach is suitable for mapping benthic substrates where high-resolution MBES data sets and suitable sediment ground-truthing are available. Other studies have found the highest POC concentrations are associated with gravelly mud, mud, and sandy mud (Diesing *et al.*, 2017). This agrees with our linear regression that areas of increased OC have a high mud content (Figure 4). The
415 empirical relationship observed between mud content and OC strongly suggests the importance of using substrate maps to precisely estimate the stock of OC.

5.2 Variability in Organic Carbon Stocks

Differences in estimated OC stock suggest that the substrate map was an essential component to this study. Smeaton *et al.* (2021) note that the seafloor is commonly assumed homogenous in benthic OC studies. Shelf
420 environments are inherently heterogeneous, and scaling up OC measurements where high-resolution mapping data are available offers an effective way of obtaining accurate estimates of OC in these areas (Snelgrove *et al.*, 2018). To improve estimates and better identify how the ocean carbon cycle will be altered by climate change and possibly human activities, carbon studies should embrace the full complexity of the seafloor (Snelgrove *et al.*, 2018; Epstein *et al.*, 2023). Our study emphasizes the benefits of high resolution MBES data for such applications, and the need
425 for additional coverage and collection of seafloor mapping data sets in coastal waters where coverage is currently limited (Mayer *et al.*, 2018).

The difference in the total m_{oc} calculated based on the substrate map (16,437 and 6,475 t of OC) versus estimates in the absence of a map (80,901 and 58,406 t of OC) emphasizes that a spatial component to OC estimations is essential for carbon system models. This difference demonstrates the need to understand the presence of hard
430 substrate at the seabed when calculating carbon stocks as suggested in recent broadscale carbon modelling studies (Epstein *et al.*, 2023). Currently, global carbon models are oversimplifying carbon processes due to a lack of information and data on the complexity of the marine carbon cycle. For instance, previous studies have examined

carbon quantity at the surface of the oceans by analyzing phytoplankton activity using satellite imagery, since there is an assumption that carbon at the surface of the oceans correlates with areas of high carbon storage at the
435 seafloor (Chase *et al.*, 2022). This assumption ignores the complexity of carbon moving through the pelagic and benthic regions. Spatially continuous seafloor mapping data are a step towards improving accuracy in our estimation, which will enhance the ongoing investigations into the marine carbon cycle.

Additionally, the resolution of the seafloor mapping data is important when modeling OC. For instance, by using a 2-by-2 m grid resolution we can interpolate the carbon within the soft substrate using EBRK models. Through
440 the EBRK interpolation of carbon, the carbon stock (6,389 Mt of OC) was less than the estimates that assume a homogenous soft substrate. The EBRK method indicates that high resolution interpolated models of OC can help to further refine standing stock estimates and provide insight into where the carbon hotspots are within the study area.

The estimates from our study were compared to the paper by Epstein *et al.* (2024) since they evaluated organic
445 carbon stock in the entire Canadian continental margin, which included our study area. To compare these estimates, we clipped their OC density map to our study site and found that the mean OC density was 7.12 kg/m^3 (3.89 kg/m^3 to 11.6 kg/m^3). This mean OC density is within the range of scenarios 1, 3 (0.804 kg/m^3 to 14.31 kg/m^3), and 4 (0 kg/m^3 to 7.91 kg/m^3) presented here. To compare the total OC stock for the study region, we adjusted the depth used by Epstein *et al.* (2024) from 0.3 m to 0.1 m by dividing their OC stock estimates by 3. The OC stock was
450 $161,552 \text{ t}$ ($88,183 \text{ t}$ to $263,076 \text{ t}$), which is within the range of scenario 1 ($17,949 \text{ t}$ to $319,335 \text{ t}$). One reason for the higher estimates in the study by Epstein *et al.* (2024) could be that no OC measurements within the study region were available in Epstein *et al.* (2024). Therefore, their model relied on OC data outside this area, which could lead to error. Furthermore, an underrepresentation of zero values in the response data, could lead to an overestimation of organic carbon standing stocks in their study, as zero values are unlikely to be predicted from
455 model outputs. The comparison between both studies highlights the importance of sediment classification maps when estimating sedimentary OC stock; knowing the extent of bedrock can reduce the overestimation of OC content substantially.

5.3 Organic Carbon Maps

When comparing the EBK and the EBRK carbon maps, there were some similarities and differences. Both maps
460 indicate a hotspot near Owls Head Harbour and low OC density on the eastern side of the study area. Yet, the EBK map shows a large area of high OC density on the west side of the study area, whereas the EBRK model has a smaller area slightly east of that location. These differences between the models emphasize that the EBK model could have some inaccurate interpolation due to the limited sediment samples in the study area. In contrast, the EBRK model was performed in the soft substrate, where all the samples were distributed, with fewer data gaps.
465 The EBK model indicates that without high-resolution seafloor mapping data, you can obtain a general understanding of OC hotspots. However, the EBRK model can provide a more precise understanding of the spatial variability of OC density in the study site.

Both maps suggest high OC densities associated with locations further offshore (Figures 9 & 10) and within sediments containing increased amounts of silt and sand (Figures 7 & 8). Based on previous evaluations of the study area, inshore sediment is often comprised of bedrock with patchy sand and gravel, whereas further offshore, there is thick glacial marine mud over bedrock (Fisheries and Oceans Canada, 2019). This geomorphology could be the cause of higher OC density further offshore. The cause of increased OC content near Owls Head Harbour remains uncertain, lacking any aquaculture or substantial runoff from nearby agriculture. However, the ESI has substantial kelp and eelgrass beds; future research may explore relationships between these environments and OC.

475 **5.4 Limitations of the Study**

The lack of dry bulk density measurements for the OC stock calculations was a major limitation of this study. The use of a dry bulk density equation derived from a previous study could introduce error into calculations based on regional geological differences. Only two seabed sediment classes were mapped here, which does not represent the actual complexity of substrate types within the ESI. Preliminary Random Forest model runs that incorporated additional sediment classes showed high error and poor performance, likely due to the difficulty in accurately determining sediment types from a small number of subsea video samples. We emphasize challenges associated with differentiating complex substrate classes that have been noted in previous similar studies (e.g., Diesing *et al.*, 2020).

We have also assumed here that there is no OC in the hard substrate. The hard substrate class included more than bedrock, with regions of mixed sediment such as gravelly mud, visible in the subsea video which could contain some OC content. Thus, improving the sediment classification map to include more complex substrates could improve the OC stock estimates further. The limited number of OC samples may have skewed the interpolation since the data points were not uniformly distributed within the areas of soft substrate. We therefore recommend higher sampling densities for future OC studies.

490 These limitations highlight the challenges of carbon modelling on the seafloor and the need for further research into evaluating the correct procedure for utilizing sediment classification maps when predicting OC stock. Furthermore, there is persistent uncertainty surrounding how much surface particulate OC (POC) reaches the seafloor and the spatial distribution of the sinks of this material. Thus, future carbon studies should evaluate benthic-pelagic coupling and the impact it has on OC stocks.

495 **5.5 Future Implications of Organic Carbon Models**

Marine spatial planners are trying to manage the seabed in a sustainable manner and high resolution regional-scale OC mapping data could be a practical option to help identify vulnerable C stores and hotspots, and to determine how these areas may be altered due to environmental change and anthropogenic activities (Hunt *et al.*, 2021). MPAs have been defined as regions that conserve marine resources, ecosystem services or cultural heritage (Mayr *et al.*, 2010). High-resolution seafloor OC models could help redefine MPAs and allow them to incorporate areas

of high carbon stock. It is important to recognize sediments as long-term carbon sinks that provide climate regulation services.

It is challenging to measure how human activities like bottom trawling are impacting the seabed and how they influence OC without an understanding of the natural processes of marine carbon cycling. Studies that examine OC spatially and its connections to seafloor composition are a crucial component to piecing together the natural marine carbon cycle, which can help determine if the amount of remineralization occurring from human activities will have a substantial impact on climate. Even with a relatively limited number of OC samples, this study demonstrates that high-resolution seafloor substrate maps and spatial OC models are critical to understanding the spatial heterogeneity of OC on the seafloor.

510 **6 Conclusions**

In this study, we generated a high-resolution sediment map that accurately captured the spatial complexity and distribution of broad sediment types in the ESI area. Through the four scenarios for estimating OC stocks, we demonstrated that seafloor sediments are a good high-resolution proxy that enable accurate estimation of OC stock in the area, and that information (or lack of information) regarding the spatial heterogeneity of the seafloor substrata substantially influences estimates of OC stock (ranging from 80,901 – 6,475 t of OC). These results emphasize that further research should explore high-resolution multibeam echosounder data in determining OC rich hotspots to improve our understanding of the role that benthic systems play as global carbon stores, and how management of these systems can contribute towards climate change management strategies and marine climate policy.

520 **Data Availability**

Bathymetry data was obtained from the Canadian Hydrographic Service (CHS) NONNA Portal [-https://data.chs-shc.ca/login](https://data.chs-shc.ca/login). All other data used in this study is in the supplementary material or available upon reasonable request.

Competing Interests

One of the authors is a member of the editorial board of *Biogeosciences*.

525 **References**

Acharya, S. S., & Panigrahi, M. K. (2016). Evaluation of factors controlling the distribution of organic matter and phosphorus in the Eastern Arabian Shelf: A geostatistical reappraisal. *Continental Shelf Research*, 126, 79–88. <https://doi.org/10.1016/j.csr.2016.08.001>

- ArcGIS Pro. (2023). *Focal Statistics (spatial analyst)*. Focal Statistics (Spatial Analyst)-ArcGIS Pro | Documentation.
530 <https://pro.arcgis.com/en/pro-app/latest/tool-reference/spatial-analyst/focal-statistics.htm>
- Atwood, T. B., Witt, A., Mayorga, J., Hammill, E., & Sala, E. (2020). Global Patterns in Marine Sediment Carbon Stocks. *Frontiers in Marine Science*, 7, 165. <https://doi.org/10.3389/fmars.2020.00165>
- Berner, R.A. (2003) 'The long-term carbon cycle, fossil fuels and atmospheric composition', *Nature*, 426, pp. 323–
535 326. Available at: <https://doi.org/10.1038/nature02131>. Bianchi, T.S., Aller, R.C., Atwood, T.B., Brown, C.J., Buatois, L.A., Levin, L.A., Levinton, J.S., Middelburg, J.J., Morrison, E.S., Regnier, P., Shields, M.R., Snelgrove, P.V., Sotka, E.E., & Stanley, R.R. (2021). What global biogeochemical consequences will marine animal–sediment interactions have during climate change? *Elementa: Science of the Anthropocene* 9: 1. doi.10.1525/elementa.2020.00180
- 540 Bianchi, T. S., Brown, C. J., Snelgrove, P. V. R., Stanley, R. R. E., Cote, D., & Morris, C. (2023). Benthic Invertebrates on the Move: A Tale of Ocean Warming and Sediment Carbon Storage. *Limnology and Oceanography Bulletin*, 32(1), 1–5. <https://doi.org/10.1002/lob.10544>
- Bondt, G. (2019). Final Field report for the Eastern Shore Islands. CHSDIR Project Number: 2901633 1001-07-F01_2901633_2602567_EasternShore_FFR%20(1).pdf
- 545 Bondt, G. (2020). Final Field report for the Eastern Shore Islands. CHSDIR Project Number: 9000294 9000713_1001-07-F01_9000294_EasternShore_2020_Field%20Report%20(1).pdf
- Boumpoulis, V., Michalopoulou, M. & Depountis, N. (2023). Comparison between different spatial interpolation methods for the development of sediment distribution maps in coastal areas. *Earth Sci Inform* 16, 2069–2087. <https://doi.org/10.1007/s12145-023-01017-4>
- 550 Brown, C. J., Smith, S. J., Lawton, P., & Anderson, J. T. (2011). Benthic habitat mapping: A review of progress towards improved understanding of the spatial ecology of the seafloor using acoustic techniques. *Estuarine, Coastal and Shelf Science*, 92(3), 502–520. <https://doi.org/10.1016/j.ecss.2011.02.007>
- Brown, D. R., Conrad, S., Akkerman, K., Fairfax, S., Fredericks, J., Hanrio, E., Sanders, L. M., Scott, E., Skillington, A., Tucker, J., Van Santen, M. L., & Sanders, C. J. (2016). Seagrass, mangrove and saltmarsh sedimentary
555 carbon stocks in an urban estuary; Coffs Harbour, Australia. *Regional Studies in Marine Science*, 8, 1–6. <https://doi.org/10.1016/j.rsma.2016.08.005>

- Buhl-Mortensen, P., Lecours, V., & Brown, C. J. (2021). Editorial: Seafloor Mapping of the Atlantic Ocean. *Frontiers in Marine Science*, 8, 721602. <https://doi.org/10.3389/fmars.2021.721602>
- Burdige, D. J. (2007). Preservation of Organic Matter in Marine Sediments: Controls, Mechanisms, and an Imbalance in Sediment Organic Carbon Budgets? *Chemical Reviews*, 107(2), 467–485. <https://doi.org/10.1021/cr050347q>
- Chase, A. P., Boss, E. S., Haëntjens, N., Culhane, E., Roesler, C., & Karp-Boss, L. (2022). Plankton Imagery Data Inform Satellite-Based Estimates of Diatom Carbon. *Geophysical Research Letters*, 49(13). <https://doi.org/10.1029/2022GL098076>
- Collier, J. S., and Brown, C. J. (2005). Correlation of sidescan backscatter with grain size distribution of surficial seabed sediments. *Mar. Geol.* 214, 431–449. doi: 10.1016/j.margeo.2004.11.011
- Dahl, M, Deyanova, D, Gütschow, S, Asplund, ME, Lyimo, LD, et al. (2016) Sediment Properties as Important Predictors of Carbon Storage in *Zostera marina* Meadows: A Comparison of Four European Areas. *PLOS ONE* 11(12): e0167493. <https://doi.org/10.1371/journal.pone.0167493>
- Diesing, M., Kröger, S., Parker, R., Jenkins, C., Mason, C., & Weston, K. (2017). Predicting the standing stock of organic carbon in surface sediments of the North–West European continental shelf. *Biogeochemistry*, 135(1–2), 183–200. <https://doi.org/10.1007/s10533-017-0310-4>
- Diesing, M., Mitchell, P.J., O’Keeffe, E., Gavazzi, G.O.A.M., Bas, T.L. (2020). Limitations of Predicting Substrate Classes on a Sedimentary Complex but Morphologically Simple Seabed. *Remote Sensing* 12, 3398. <https://doi.org/10.3390/rs12203398>
- Diesing, M., Thorsnes, T., and Bjarnadóttir, L. R. (2021). Organic carbon densities and accumulation rates in surface sediments of the North Sea and Skagerrak, *Biogeosciences*, 18, 2139–2160, <https://doi.org/10.5194/bg-18-2139-2021>, 2021.
- Epstein, G., Middelburg, J. J., Hawkins, J. P., Norris, C. R., & Roberts, C. M. (2022). The impact of mobile demersal fishing on carbon storage in seabed sediments. *Global Change Biology*, 28(9), 2875–2894. <https://doi.org/10.1111/gcb.16105>
- Epstein, G., Fuller, S. D., Hingmire, D., Myers, P. G., Peña, A., Pennelly, C., and Baum, J. K. (2024). Predictive mapping of organic carbon stocks in surficial sediments of the Canadian continental margin, *Earth Syst. Sci. Data*, 16, 2165–2195, <https://doi.org/10.5194/essd-16-2165-2024>.

- 585 Feng, T., Stanley, R. R. E., Wu, Y., Kenchington, E., Xu, J., & Horne, E. (2022). A High-Resolution 3-D Circulation Model in a Complex Archipelago on the Coastal Scotian Shelf. *Journal of Geophysical Research. Oceans*, 127(3). <https://doi.org/10.1029/2021JC017791>
- Fennel, K., Alin, S., Barbero, L., Evans, W., Bourgeois, T., Cooley, S., Dunne, J., Feely, R. A., Hernandez-Ayon, J. M., Hu, X., Lohrenz, S., Muller-Karger, F., Najjar, R., Robbins, L., Shadwick, E., Siedlecki, S., Steiner, N.,
- 590 Sutton, A., Turk, D., ... Wang, Z. A. (2019). Carbon cycling in the North American coastal ocean: A synthesis. *Biogeosciences*, 16(6), 1281–1304. <https://doi.org/10.5194/bg-16-1281-2019>
- Fisheries and Oceans Canada (2019). Biophysical and Ecological Overview of the Eastern Shore Islands Area of Interest (AOI). DFO Can. Sci. Advis. Sec. Sci. Advis. Rep. 2019/016.
- 595 Giustini, F., Ciotoli, G., Rinaldini, A., Ruggiero, L., & Voltaggio, M. (2019). Mapping the geogenic radon potential and radon risk by using Empirical Bayesian Kriging regression: A case study from a volcanic area of central Italy. *The Science of the Total Environment*, 661, 449–464. <https://doi.org/10.1016/j.scitotenv.2019.01.146>
- Goff, J. A., Olson, H. C., and Duncan, C. S. (2000). Correlation of side-scan backscatter intensity with grain-size distribution of shelf sediments, New Jersey margin. *Geo Mar. Lett.* 20, 43–49. doi: 10.1007/s003670000032
- 600 Haar, C.D., Misiuk, B., Gazzola, V., Wells, M., Brown, C.J. (2023). Harmonizing multi-source backscatter data to generate regional seabed maps: Bay of Fundy, Canada. *Journal of Maps*. 19 (1) doi.10.1080/17445647.2023.222362
- Hedges, J. I., & Keil, R. G. (1995). Sedimentary organic matter preservation: An assessment and speculative synthesis. *Marine Chemistry*.
- 605 Hilborn, R., Amoroso, R., Collie, J., Hiddink, J. G., Kaiser, M. J., Mazor, T., McConnaughey, R. A., Parma, A. M., Pitcher, C. R., Sciberras, M., & Suuronen, P. (2023). Evaluating the sustainability and environmental impacts of trawling compared to other food production systems. *ICES Journal of Marine Science*, fsad115. <https://doi.org/10.1093/icesjms/fsad115>
- Hilmi, N., Chami, R., Sutherland, M. D., Hall-Spencer, J. M., Lebleu, L., Benitez, M. B., & Levin, L. A. (2021). The
- 610 Role of Blue Carbon in Climate Change Mitigation and Carbon Stock Conservation. *Frontiers in Climate*, 3, 710546. <https://doi.org/10.3389/fclim.2021.710546>

- Howard, J., Sutton-Grier, A. E., Smart, L. S., Lopes, C. C., Hamilton, J., Kleypas, J., Simpson, S., McGowan, J., Pessarrodona, A., Alleway, H. K., and Landis, E. (2023). Blue Carbon pathways for climate mitigation: Known, emerging and unlikely, *Mar Policy*, 156, 105788, <https://doi.org/https://doi.org/10.1016/j.marpol.2023.105788>, 2023.
- 615
- Huang, Z., Nichol, S. L., Siwabessy, J. P., Daniell, J., & Brooke, B. P. (2012). Predictive modelling of seabed sediment parameters using multibeam acoustic data: a case study on the Carnarvon Shelf, Western Australia. *International Journal of Geographical Information Science*, 26(2), 283-307.
- Hunt, C. A., Demšar, U., Marchant, B., Dove, D., & Austin, W. E. N. (2021). Sounding Out the Carbon: The Potential of Acoustic Backscatter Data to Yield Improved Spatial Predictions of Organic Carbon in Marine Sediments. *Frontiers in Marine Science*, 8, 756400. <https://doi.org/10.3389/fmars.2021.756400>
- 620
- Hunt, C., Demšar, U., Dove, D., Smeaton, C., Cooper, R., & Austin, W. E. N. (2020). Quantifying Marine Sedimentary Carbon: A New Spatial Analysis Approach Using Seafloor Acoustics, Imagery, and Ground-Truthing Data in Scotland. *Frontiers in Marine Science*, 7, 588. <https://doi.org/10.3389/fmars.2020.00588>
- 625
- IPCC. (2019). Annex I: Glossary [Weyer, N.M. (ed.)]. In: IPCC Special Report on the Ocean and Cryosphere in a Changing Climate [H.-O. Pörtner, D.C. Roberts, V. Masson-Delmotte, P. Zhai, M. Tignor, E. Poloczanska, K. Mintenbeck, A. Alegría, M. Nicolai, A. Okem, J. Petzold, B. Rama, N.M. Weyer (eds.)]. Cambridge University Press, Cambridge, UK and New York, NY, USA, pp. 677–702. <https://doi.org/10.1017/9781009157964.010>.
- 630
- Jenkins C (2005) Summary of the on-CALCULATION methods used in dbSEABED. <http://pubs.usgs.gov/ds/2006/146/docs/onCALCULATION.pdf>. Accessed 27 July 2023
- Krause, J.R., Hinojosa-Corona, A., Gray, A.B., Herguera, J.C., McDonnell, J., Schaefer, M.V., Ying, S.C., Watson, E.B. (2022). Beyond habitat boundaries: Organic matter cycling requires a system-wide approach for accurate blue carbon accounting. *Limnology and Oceanography*. 9999: 1-13. doi: 10.1002/lno.12071
- 635
- King, E. L. (2018). *Surficial geology and features of the inner shelf of eastern shore, offshore Nova Scotia* (8375; p. 8375). <https://doi.org/10.4095/308454>
- Krivoruchko K, Gribov A. (2019). Evaluation of empirical Bayesian kriging. *Spat Stat* 32: <https://doi.org/10.1016/j.spasta.2019.100368>

- Legge, O., Johnson, M., Hicks, N., Jickells, T., Diesing, M., Aldridge, J., Andrews, J., Artioli, Y., Bakker, D. C. E.,
640 Burrows, M. T., Carr, N., Cripps, G., Felgate, S. L., Fernand, L., Greenwood, N., Hartman, S., Kröger, S.,
Lessin, G., Mahaffey, C., ... Williamson, P. (2020). Carbon on the Northwest European Shelf: Contemporary
Budget and Future Influences. *Frontiers in Marine Science*, 7, 143.
<https://doi.org/10.3389/fmars.2020.00143>
- Liaw, A., Wiener, M.. (2002). Classification and regression by randomForest. *R news* 2, 18–22.
- 645 Lovelock, C. E. and Duarte, C. M. (2019). Dimensions of Blue Carbon and emerging perspectives, *Biol Lett*, 15,
20180781, <https://doi.org/10.1098/rsbl.2018.0781>, 2019.
- Lucieer, V., Hill, N. A., Barrett, N. S., & Nichol, S. (2013). Do marine substrates ‘look’and ‘sound’the same?
Supervised classification of multibeam acoustic data using autonomous underwater vehicle
images. *Estuarine, Coastal and Shelf Science*, 117, 94-106.
- 650 Mallik, S., Bhowmik, T., Mishra, U., & Paul, N. (2022). Mapping and prediction of soil organic carbon by an advanced
geostatistical technique using remote sensing and terrain data. *Geocarto International*, 37(8), 2198–2214.
<https://doi.org/10.1080/10106049.2020.1815864>
- Mason C. (2011). NMBAQC’s Best Practice Guidance. Particle Size Analysis (PSA) for Supporting Biological
Analysis. National Marine Biological AQC Coordinating Committee.
- 655 Mayer, L., Jakobsson, M., Allen, G., Dorschel, B., Falconer, R., Ferrini, V., Lamarche, G., Snaith, H., Weatherall, P.
(2018). The Nippon Foundation—GEBCO Seabed 2030 Project: The Quest to See the World’s Oceans
Completely Mapped by 2030. *Geosciences*. 8(2):63. doi:10.3390/geosciences8020063.
- Mayr, F. B., Upton, H. F. (Harold F., Buck, E. H., Upton, H. F. (Harold F., & Vann, A. (2010). *Marine protected areas*.
Nova Science Publishers.
- 660 McHugh ML. Interrater reliability: the kappa statistic. *Biochem Med (Zagreb)*. 2012;22(3):276-82. PMID: 23092060;
PMCID: PMC3900052.
- McLeod, E. *et al.* (2011) ‘A blueprint for Blue Carbon: Toward an improved understanding of the role of vegetated
coastal habitats in sequestering CO₂’, *rontiers in Ecology and the Environment*, 9(10), pp. 552–560.
Available at: <https://doi.org/10.1890/110004>.
- 665 Middelburg, JJ. (2018). Reviews and syntheses: To the bottom of carbon processing at the seafloor. *Biogeosciences*
15: 413–427. DOI: <http://dx.doi.org/10.5194/bg-15-413-2018>.

- Misiuk, B., Brown, C.J. 2024. Benthic habitat mapping: A review of three decades of mapping biological patterns on the seafloor. *Estuarine, Coastal and Shelf Science*, 296: 108599. doi.org/10.1016/j.ecss.2023.108599
- 670 Misiuk, B., Brown, C.J., Robert, K., Lacharite, M. (2020). Harmonizing multi-source sonar backscatter datasets for seabed mapping using bulk shift approaches. *Remote Sensing*, 12(4): 601. <https://doi.org/10.3390/rs12040601>
- Misiuk, B., Diesing, M., Aitken, A., Brown, C. J., Edinger, E. N., & Bell, T. (2019). A spatially explicit comparison of quantitative and categorical modelling approaches for mapping seabed sediments using random forest. *Geosciences (Basel)*, 9(6), 254–. <https://doi.org/10.3390/geosciences9060254>
- 675 Misiuk, B., Lacharité, M., Brown, C.J. (2021). Assessing the use of harmonized multisource backscatter data for thematic benthic habitat mapping. *Science of Remote Sensing*, 3. doi.10.1016/j.srs.2021.1000
- Mitchell, P. J., Aldridge, J., & Diesing, M. (2019). Legacy data: How decades of seabed sampling can produce robust predictions and versatile products. *Geosciences (Basel)*, 9(4), 182–. <https://doi.org/10.3390/geosciences9040182>
- 680 Mollenhauer G, Schneider RR, Jennerjahn T *et al* (2004). Organic carbon accumulation in the South Atlantic Ocean: its modern, mid-Holocene and last glacial distribution. *Glob Planet C*
- Najjar, R. G., Herrmann, M., Alexander, R., Boyer, E. W., Burdige, D. J., Butman, D., Cai, W. -J., Canuel, E. A., Chen, R. F., Friedrichs, M. A. M., Feagin, R. A., Griffith, P. C., Hinson, A. L., Holmquist, J. R., Hu, X., Kemp, W. M., Kroeger, K. D., Mannino, A., McCallister, S. L., ... Zimmerman, R. C. (2018). Carbon Budget of Tidal
685 Wetlands, Estuaries, and Shelf Waters of Eastern North America. *Global Biogeochemical Cycles*, 32(3), 389–416. <https://doi.org/10.1002/2017GB005790>
- Oceans North. (2024). Mapping Carbon in Canada's Seafloor. https://www.oceansnorth.org/wp-content/uploads/2024/05/Seabed-Mapping-Policy-Brief-May2024_final2.pdf
- Pellicone G, Caloiero T, Modica G, Guagliardi I. (2018). Application of several spatial interpolation techniques to
690 monthly rainfall data in the Calabria region (southern Italy). *Int J Climatol* 38:3651–3666. <https://doi.org/10.1002/joc.5525>
- Sala, E., Mayorga, J., Bradley, D., Cabral, R. B., Atwood, T. B., Auber, A., Cheung, W., Costello, C., Ferretti, F., Friedlander, A. M., Gaines, S. D., Garilao, C., Goodell, W., Halpern, B. S., Hinson, A., Kaschner, K., Kesner-

- Reyes, K., Leprieux, F., McGowan, J., ... Lubchenco, J. (2021). Protecting the global ocean for biodiversity, food and climate. *Nature*, 592(7854), 397–402. <https://doi.org/10.1038/s41586-021-03371-z>
- 695
- Serrano, O., Lavery, P. S., Duarte, C. M., Kendrick, G. A., Calafat, A., York, P. H., Steven, A., and Macreadie, P. I. (2016). Can mud (silt and clay) concentration be used to predict soil organic carbon content within seagrass ecosystems?, *Biogeosciences*, 13, 4915–4926, <https://doi.org/10.5194/bg-13-4915-2016>, 2016.
- Smeaton, D. G., & Snellen, M. (2009). A Bayesian approach to seafloor classification using multi-beam echo-sounder backscatter data. *Applied Acoustics*, 70(10), 1258-1268.
- 700
- Smeaton, C., & Austin, W. E. N. (2019). Where's the Carbon: Exploring the Spatial Heterogeneity of Sedimentary Carbon in Mid-Latitude Fjords. *Frontiers in Earth Science*, 7, 269. <https://doi.org/10.3389/feart.2019.00269>
- Smeaton, C., Yang, H., & Austin, W. E. N. (2021). Carbon burial in the mid-latitude fjords of Scotland. *Marine Geology*, 441, 106618. <https://doi.org/10.1016/j.margeo.2021.106618>
- 705
- Snelgrove, P. V. R., Soetaert, K., Solan, M., Thrush, S., Wei, C.-L., Danovaro, R., Fulweiler, R. W., Kitazato, H., Ingole, B., Norkko, A., Parkes, R. J., & Volkenborn, N. (2018). Global Carbon Cycling on a Heterogeneous Seafloor. *Trends in Ecology & Evolution*, 33(2), 96–105. <https://doi.org/10.1016/j.tree.2017.11.004>
- Sokal RR, Rohlf FJ. (1981). *Biometry*. San Francisco, USA
- Stephens, D., & Diesing, M. (2014). A comparison of supervised classification methods for the prediction of substrate type using multibeam acoustic and legacy grain-size data. *PloS one*, 9(4), e93950.
- 710
- Stephens, D., & Diesing, M. (2015). Towards quantitative spatial models of seabed sediment composition. *PloS One*, 10(11), e0142502–e0142502. <https://doi.org/10.1371/journal.pone.0142502>
- Sutherland, T. F., Galloway, J., Loschiavo, R., Levings, C. D., and Hare, R. (2007). Calibration techniques and sampling resolution requirements for groundtruthing multibeam acoustic backscatter (EM3000) and QTC VIEW™ classification technology. *Estuar. Coast. Shelf Sci.* 75, 447–458. doi: 10.1016/j.ecss.2007.05.045
- 715
- Vandermeulen, H. (2018). *A Drop Camera Survey of the Eastern Shore Archipelago, Nova Scotia*. Canadian Technical Report of Fisheries and Aquatic Sciences 3258. https://publications.gc.ca/collections/collection_2018/mpo-dfo/Fs97-6-3258-eng.pdf
- Verardo, D. J., Froelich, P. N., & McIntyre, A. (1990). Determination of organic carbon and nitrogen in marine sediments using the Carlo Erba NA-1500 analyzer. *Deep Sea Research Part A. Oceanographic Research Papers*, 37(1), 157–165. [https://doi.org/10.1016/01980149\(90\)90034-S](https://doi.org/10.1016/01980149(90)90034-S)
- 720